



A Space-time Adaptive, Higher-order Finite Element Method for Sonic Boom

R. Trono Figueras

David L. Darmofal, Marshall C. Galbraith, Steven R. Allmaras

MIT, Department of Aeronautics and Astronautics

Funded by NASA (#80NSSC22K0193)

April 11, 2025

Motivation For Sonic Boom Study

Ultimate goal:

Enable supersonic commercial flights overland.



Source: lockheedmartin.com

Motivation For Sonic Boom Study

Ultimate goal:

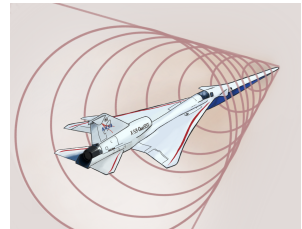
Enable supersonic commercial flights overland.

Main challenge:

- Negative impact of sonic boom loudness on humans, other animals, and structures.



Source: lockheedmartin.com



Source: michigandaily.com

Motivation For Sonic Boom Study

Ultimate goal:

Enable supersonic commercial flights overland.

Main challenge:

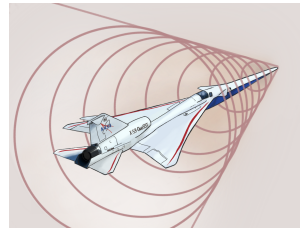
- Negative impact of sonic boom loudness on humans, other animals, and structures.

Study sonic boom to:

- Predict loudness sensitivities to airplane geometry.
- Perform airplane shape optimization to reduce loudness at ground.



Source: lockheedmartin.com



Source: michigandaily.com

Solution Approach: Broad Picture

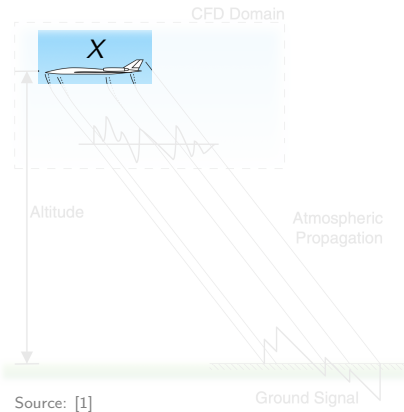
Multidisciplinary design optimization¹:

¹D. L. Rodriguez et. al. 2025

Solution Approach: Broad Picture

Multidisciplinary design optimization¹:

- Parametric geometry generator.

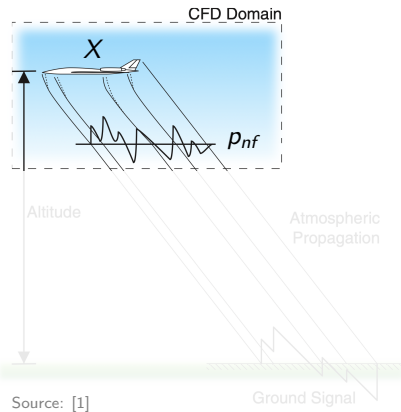


¹D. L. Rodriguez et. al. 2025

Solution Approach: Broad Picture

Multidisciplinary design optimization¹:

- Parametric geometry generator.
- CFD solver.
 - Euler/Navier-Stokes in 3D.
 - Uniform atmosphere.

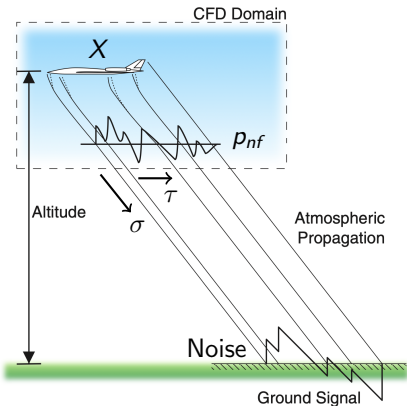


¹D. L. Rodriguez et. al. 2025

Solution Approach: Broad Picture

Multidisciplinary design optimization¹:

- Parametric geometry generator.
- CFD solver.
 - Euler/Navier-Stokes in 3D.
 - Uniform atmosphere.
- *Sonic boom propagation tool*
 - 2D problem.
 - Weakly non-linear.
 - Species relaxation.
 - Non-uniform atmosphere.

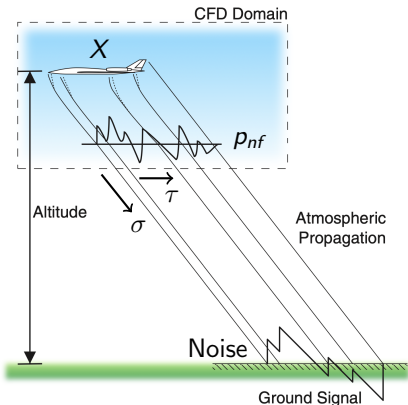


¹D. L. Rodriguez et. al. 2025

Solution Approach: Broad Picture

Multidisciplinary design optimization¹:

- Parametric geometry generator.
- CFD solver.
 - Euler/Navier-Stokes in 3D.
 - Uniform atmosphere.
- *Sonic boom propagation tool*
 - 2D problem.
 - Weakly non-linear.
 - Species relaxation.
 - Non-uniform atmosphere.
- Numerical optimizer.



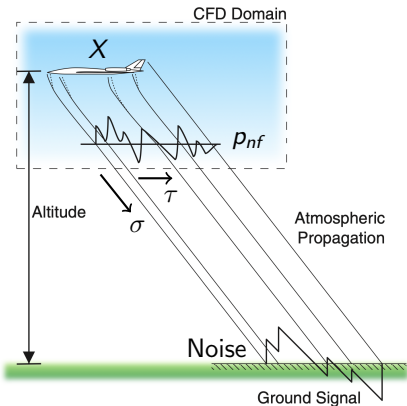
¹D. L. Rodriguez et. al. 2025

Solution Approach: Broad Picture

Multidisciplinary design optimization¹:

- Parametric geometry generator.
- CFD solver.
 - Euler/Navier-Stokes in 3D.
 - Uniform atmosphere.
- *Sonic boom propagation tool*
 - 2D problem.
 - Weakly non-linear.
 - Species relaxation.
 - Non-uniform atmosphere.
- Numerical optimizer.

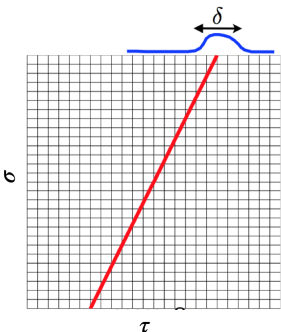
Compute noise at ground and



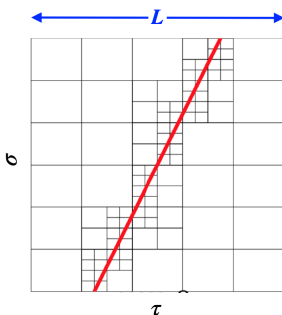
$$\frac{d(\text{Noise})}{dX} = \frac{\frac{d(\text{Noise})}{dp_{nf}} \frac{dp_{nf}}{dX}}{dp_{nf}} .$$

¹D. L. Rodriguez et. al. 2025

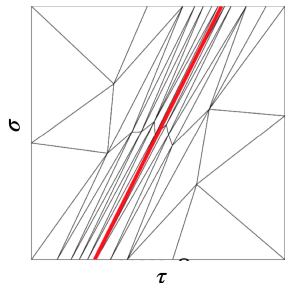
Propagation Problem: Mesh Adaptation



$$\text{DOF} = O((L/\delta)^2)$$

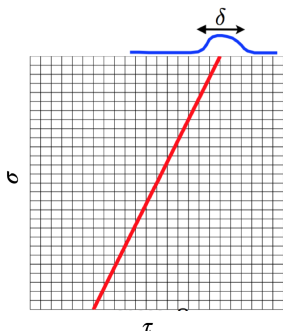


$$\text{DOF} = O(L/\delta)$$



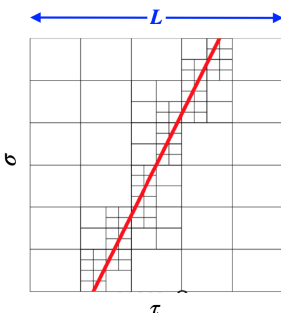
$$\text{DOF} = O(1)$$

Propagation Problem: Mesh Adaptation



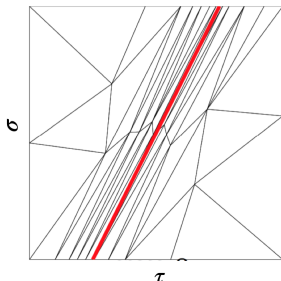
(a) uniform

$$\text{DOF} = O((L/\delta)^2)$$



(b) space-time tensor-product

$$\text{DOF} = O(L/\delta)$$



(c) space-time unstructured

$$\text{DOF} = O(1)$$

But, space-time unstructured requires 2D solve instead of marching in σ , and solving an optimization problem for the mesh.

Propagation Problem: Motivation for Mesh Adaptation

Target noise level at ground: below 75 dB.

Target noise accuracy in simulations: *reliably* at order of 0.1 dB.

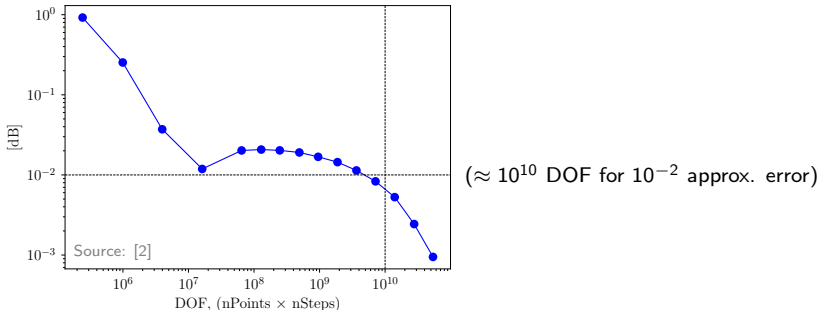
Propagation Problem: Motivation for Mesh Adaptation

Target noise level at ground: below 75 dB.

Target noise accuracy in simulations: *reliably* at order of 0.1 dB.

Results for standard time-marching methods²:

Approximate Error in Noise

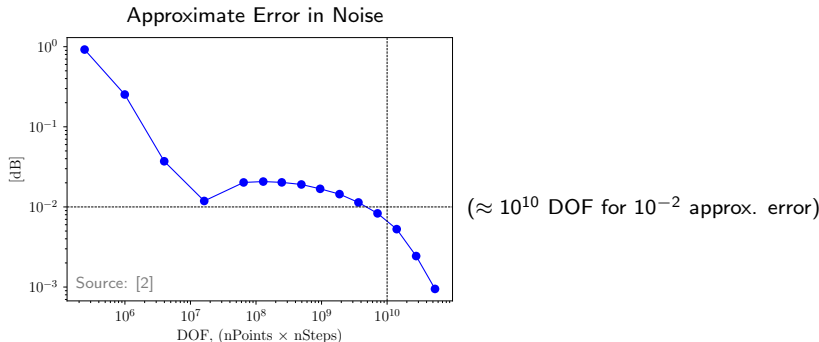


Propagation Problem: Motivation for Mesh Adaptation

Target noise level at ground: below 75 dB.

Target noise accuracy in simulations: *reliably* at order of 0.1 dB.

Results for standard time-marching methods²:



Our goal: Reduce the significant computational cost involved.

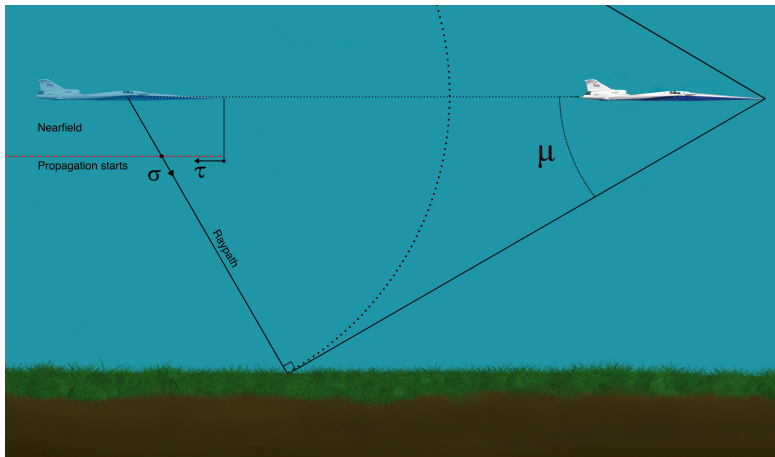
Enable efficient, automated high accuracy predictions of boom propagation and design sensitivities through adaptive control of numerical error.

²S. K. Rallabhandi et. al. 2023

Boom Propagation Modeling and Adaptive Approach

Coordinate System

Airplane at cruise altitude and cruise Mach number (M_a):



$$\text{Mach cone angle: } \mu = \sin^{-1}(1/M_a).$$

Augmented Burgers System

To model sonic boom propagation we use the augmented Burgers system of equations, for the states $(P, \tilde{P}_{O_2}, \tilde{P}_{N_2})$:

Augmented Burgers System

To model sonic boom propagation we use the augmented Burgers system of equations, for the states $(P, \tilde{P}_{O_2}, \tilde{P}_{N_2})$:

$$\frac{\partial P}{\partial \sigma} - \frac{1}{2} \frac{\partial \ln(\rho_0 c_0 / A_{n0})}{\partial \sigma} P - \frac{1}{2} \frac{\partial P^2}{\partial \tau} - \frac{1}{\Gamma} \frac{\partial^2 P}{\partial \tau^2} - \frac{\partial}{\partial \tau} \left(\sum_{\nu} C_{\nu} \frac{\partial \tilde{P}_{\nu}}{\partial \tau} \right) = 0 \text{ on } \Omega, \quad (1)$$

$$-\frac{\partial \tilde{P}_{\nu}}{\partial \tau} + \frac{P - \tilde{P}_{\nu}}{\theta_{\nu}} = 0 \text{ on } \Omega, \quad \nu = \{O_2, N_2\}, \quad (2)$$

which includes:

- Thermoviscous diffusion.
- Atmospheric absorption by relaxation species (O_2 and N_2).
- Ray tube area variation.

Augmented Burgers System

To model sonic boom propagation we use the augmented Burgers system of equations, for the states $(P, \tilde{P}_{O_2}, \tilde{P}_{N_2})$:

$$\frac{\partial P}{\partial \sigma} - \frac{1}{2} \frac{\partial \ln(\rho_0 c_0 / A_{n0})}{\partial \sigma} P - \frac{1}{2} \frac{\partial P^2}{\partial \tau} - \frac{1}{\Gamma} \frac{\partial^2 P}{\partial \tau^2} - \frac{\partial}{\partial \tau} \left(\sum_{\nu} C_{\nu} \frac{\partial \tilde{P}_{\nu}}{\partial \tau} \right) = 0 \text{ on } \Omega, \quad (1)$$

$$-\frac{\partial \tilde{P}_{\nu}}{\partial \tau} + \frac{P - \tilde{P}_{\nu}}{\theta_{\nu}} = 0 \text{ on } \Omega, \quad \nu = \{O_2, N_2\}, \quad (2)$$

which includes:

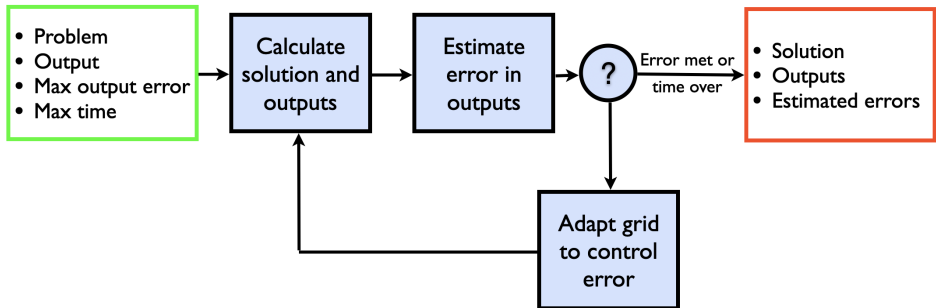
- Thermoviscous diffusion.
- Atmospheric absorption by relaxation species (O_2 and N_2).
- Ray tube area variation.

Remarks:

- Eq (1) is parabolic, with σ the time-like direction.
- It is typically solved with a time-marching scheme. **Not in our case.**

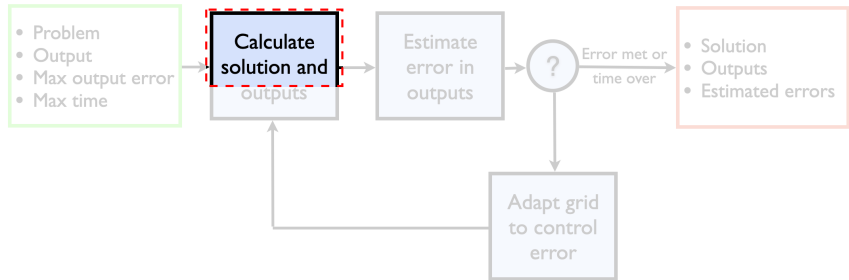
Output-based Adaptation Cycle

Adaptive cycle scheme:



Output of interest: Loudness at ground.

Discretization and Shock Capturing



Continuous Galerkin type FEM

CG weak statement:

Find $\mathbf{u}_h \in \mathcal{V}_{h,p}$ such that:

$$\mathcal{R}(\mathbf{v}_h, \mathbf{u}_h) = 0, \quad \forall \mathbf{v}_h \in \mathcal{V}_{h,p}, \quad (3)$$

where the space $\mathcal{V}_{h,p}$ contains polynomials of order p in Ω .

Continuous Galerkin type FEM

CG weak statement:

Find $\mathbf{u}_h \in \mathcal{V}_{h,p}$ such that:

$$\mathcal{R}(\mathbf{v}_h, \mathbf{u}_h) = 0, \quad \forall \mathbf{v}_h \in \mathcal{V}_{h,p}, \quad (3)$$

where the space $\mathcal{V}_{h,p}$ contains polynomials of order p in Ω .

Remarks:

- A discontinuous subscale is used for stabilization, and the resulting method is known as Variational Multiscale with Discontinuous Subscales (VMSD).
- The discretization is adjoint consistent.

The Need for Artificial Viscosity

Challenge: Discontinuities (shocks) in the solutions, leading to unstable numerical solves and lack of convergence.

The Need for Artificial Viscosity

Challenge: Discontinuities (shocks) in the solutions, leading to unstable numerical solves and lack of convergence.

Goal: Smoothen discontinuities to improve stability, while not modifying the already smooth areas.

The Need for Artificial Viscosity

Challenge: Discontinuities (shocks) in the solutions, leading to unstable numerical solves and lack of convergence.

Goal: Smoothen discontinuities to improve stability, while not modifying the already smooth areas.

Approach: Employ a shock sensor, s , to keep track of discontinuities, and use that information to add localized artificial viscosity.

The Need for Artificial Viscosity

Challenge: Discontinuities (shocks) in the solutions, leading to unstable numerical solves and lack of convergence.

Goal: Smoothen discontinuities to improve stability, while not modifying the already smooth areas.

Approach: Employ a shock sensor, s , to keep track of discontinuities, and use that information to add localized artificial viscosity.

Add extra diffusion term in Burgers equation:

$$\frac{\partial P}{\partial \sigma} - \frac{1}{2} \frac{\partial \ln(\rho_0 c_0 / A_{n0})}{\partial \sigma} P - \frac{1}{2} \frac{\partial P^2}{\partial \tau} - \frac{1}{\Gamma} \frac{\partial^2 P}{\partial \tau^2} - \frac{\partial}{\partial \tau} \left(\sum_{\nu} C_{\nu} \frac{\partial \tilde{P}_{\nu}}{\partial \tau} \right) - \underbrace{\frac{\partial}{\partial \tau} \left(\epsilon_{AV} \frac{\partial P}{\partial \tau} \right)}_{\text{extra term}} = 0, \quad (4)$$

with ϵ_{AV} as:

$$\epsilon_{AV} := \underbrace{\frac{1}{2} \frac{H_{\tau\tau}}{p} |P| s}_{AV_{\max}}. \quad (5)$$

PDE-based Shock Sensor³

Shock sensor design requirements:

- $s \approx 1$ in shock areas.
- $s \approx 0$ away from shocks, of order $\mathcal{O}(h^p)$.
- s smooth.

(6)

PDE-based Shock Sensor³

Shock sensor design requirements:

- $s \approx 1$ in shock areas.
- $s \approx 0$ away from shocks, of order $\mathcal{O}(h^P)$.
- s smooth.

Define PDE for shock sensor s :

$$\underbrace{s - C_1 s_{\text{grad}}}_{\text{source term}} = 0 \text{ on } \Omega. \quad (6)$$

- s_{grad} : **Shock indicator** based on pressure solution gradient.

PDE-based Shock Sensor³

Shock sensor design requirements:

- $s \approx 1$ in shock areas.
- $s \approx 0$ away from shocks, of order $\mathcal{O}(h^p)$.
- s smooth.

Define PDE for shock sensor s :

$$\underbrace{s - C_1 s_{\text{grad}}}_{\text{source term}} + \underbrace{C_2 \nabla \cdot \left(\frac{H^T H}{p^2} \nabla s \right)}_{\text{diffusion term}} = 0 \text{ on } \Omega. \quad (6)$$

- s_{grad} : **Shock indicator** based on pressure solution gradient.
- Diffusion term: to have a smooth sensor solution.
- H : element size field.

Shock Indicator s_{grad}

Identify pressure changes in τ direction:

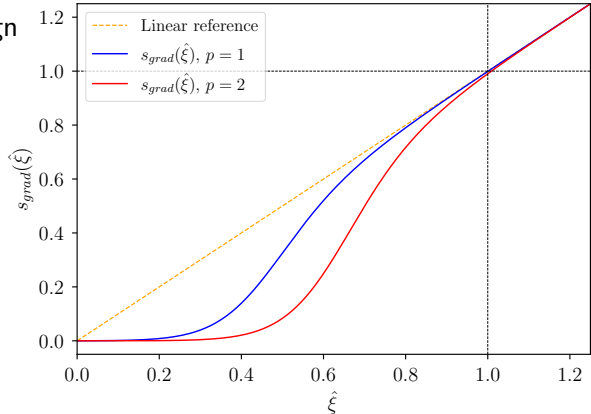
$$\xi := \frac{H_{\tau\tau}}{p} \left| \frac{\partial P}{\partial \tau} \right|, \quad \hat{\xi} := \frac{\xi}{\xi_1}, \quad (7)$$

Shock Indicator s_{grad}

Identify pressure changes in τ direction:

$$\xi := \frac{H_{\tau\tau}}{p} \left| \frac{\partial P}{\partial \tau} \right|, \quad \hat{\xi} := \frac{\xi}{\xi_1}, \quad (7)$$

Define $s_{\text{grad}}(\hat{\xi})$ to meet design requirements



Test With Smooth Problem

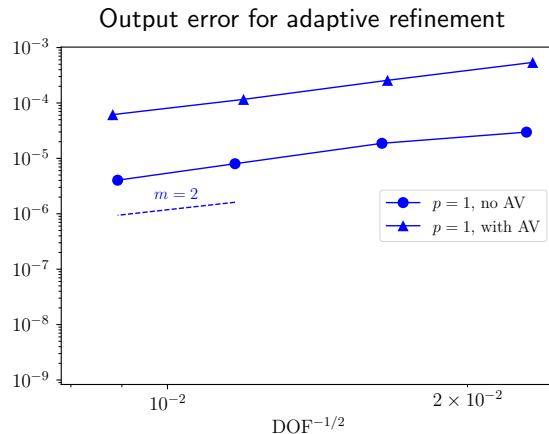
Smooth problem with available exact solution:

- Solve without artificial viscosity.
- Solve with artificial viscosity and see how it affects convergence.

Test With Smooth Problem

Smooth problem with available exact solution:

- Solve without artificial viscosity.
- Solve with artificial viscosity and see how it affects convergence.

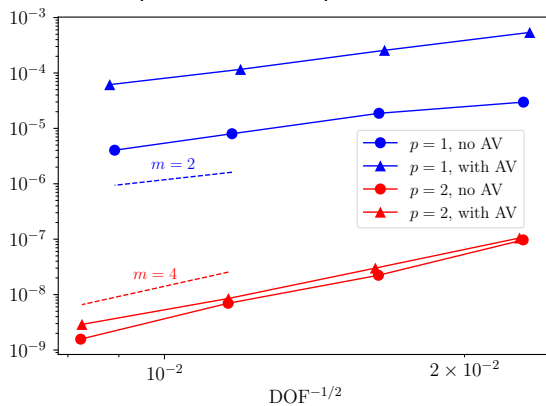


Test With Smooth Problem

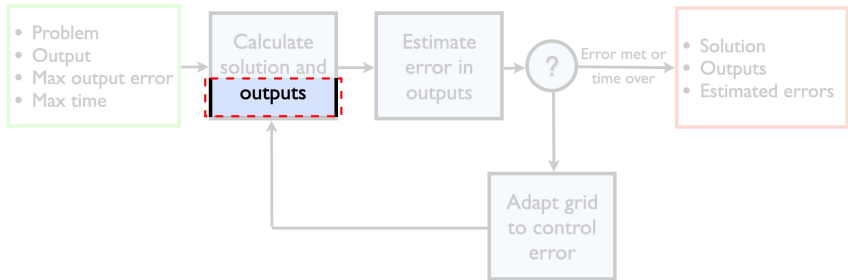
Smooth problem with available exact solution:

- Solve without artificial viscosity.
- Solve with artificial viscosity and see how it affects convergence.

Output error for adaptive refinement



Ground Signal Filtering



At Ground: Relevant Loudness Metrics

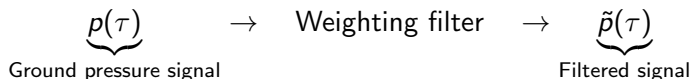
The human ear is less sensitive to low audio frequencies.

There is a family of weighting filter curves that account for this relative loudness perceived by humans: A/B/C/D/-SEL curves.

At Ground: Relevant Loudness Metrics

The human ear is less sensitive to low audio frequencies.

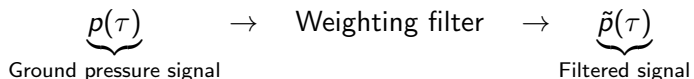
There is a family of weighting filter curves that account for this relative loudness perceived by humans: A/B/C/D/-SEL curves.



At Ground: Relevant Loudness Metrics

The human ear is less sensitive to low audio frequencies.

There is a family of weighting filter curves that account for this relative loudness perceived by humans: A/B/C/D/-SEL curves.



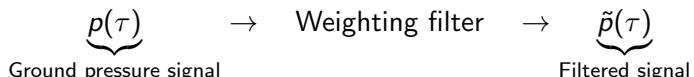
Sound exposure:

$$E = \frac{1}{\omega_{\text{ref}}} \int_{\tau_0}^{\tau_f} [\tilde{p}(\tau)]^2 d\tau. \quad (8)$$

At Ground: Relevant Loudness Metrics

The human ear is less sensitive to low audio frequencies.

There is a family of weighting filter curves that account for this relative loudness perceived by humans: A/B/C/D/-SEL curves.



Sound exposure:

$$E = \frac{1}{\omega_{\text{ref}}} \int_{\tau_0}^{\tau_f} [\tilde{p}(\tau)]^2 d\tau. \quad (8)$$

Loudness level in dB:

$$\text{Loudness} = 10 \log_{10} \left(\frac{E}{E_0} \right), \quad E_0 = 400 \text{ } (\mu\text{Pa})^2\text{s}. \quad (9)$$

B-SEL Metric

We focus on the B-SEL curve, and the approach can be generalized to any other.

B-SEL Metric

We focus on the B-SEL curve, and the approach can be generalized to any other.

Transfer function in the complex frequency (χ) domain:

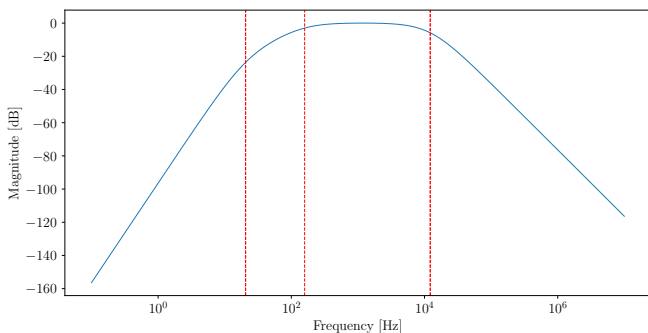
$$H_B(\chi) = \frac{\tilde{P}(\chi)}{P(\chi)} = \frac{c_B \chi^3}{(\chi + 2\pi f_1)^2 (\chi + 2\pi f_{2B}) (\chi + 2\pi f_4)^2}, \quad (10)$$

B-SEL Metric

We focus on the B-SEL curve, and the approach can be generalized to any other.

Transfer function in the complex frequency (χ) domain:

$$H_B(\chi) = \frac{\tilde{P}(\chi)}{P(\chi)} = \frac{c_B \chi^3}{(\chi + 2\pi f_1)^2 (\chi + 2\pi f_{2B})(\chi + 2\pi f_4)^2}, \quad (10)$$



Filter Application at Ground: ODE Approach

Common filtering techniques not suitable for our unstructured grid.

Filter Application at Ground: ODE Approach

Common filtering techniques not suitable for our unstructured grid.

Convert transfer function in complex frequency domain:

$$\tilde{P}(\chi) = P(\chi) \frac{K\chi^3}{(\chi + a)^2(\chi + b)(\chi + c)^2}, \quad (11)$$

to a **system of ODE's** in the τ domain (to solve in *ground* boundary):

Filter Application at Ground: ODE Approach

Common filtering techniques not suitable for our unstructured grid.

Convert transfer function in complex frequency domain:

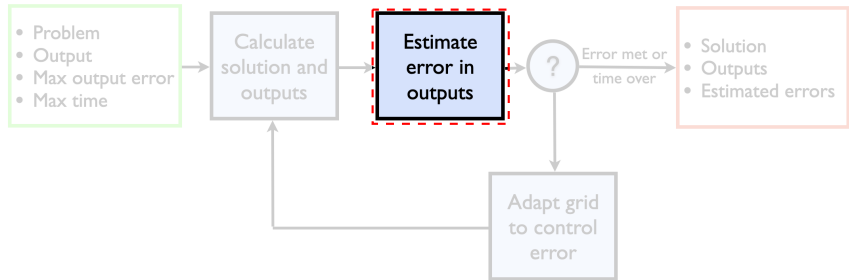
$$\tilde{P}(\chi) = P(\chi) \frac{K\chi^3}{(\chi + a)^2(\chi + b)(\chi + c)^2}, \quad (11)$$

to a **system of ODE's** in the τ domain (to solve in *ground* boundary):

$$\frac{d\bar{u}}{d\tau} = \begin{pmatrix} 0 & 1 & 0 & 0 & 0 \\ -a^2 & -2a & 0 & 0 & 0 \\ 0 & 0 & 0 & 1 & 0 \\ -K^{1/3}a^2 & -2K^{1/3}a & -c^2 & -2c & 0 \\ 0 & 0 & 0 & K^{1/3} & -b \end{pmatrix} \bar{u} + \begin{pmatrix} 0 \\ K^{1/3}p(\tau) \\ 0 \\ K^{2/3}p(\tau) \\ 0 \end{pmatrix}, \quad (12)$$

where $\bar{u} = (u_0, u_1, u_2, u_3, \tilde{p})^T$, with homogeneous initial conditions.

Output Error Estimation



Output Functional and Error

We consider the following output functional:

$$\mathcal{J}(\mathbf{u}) := \int_{\text{ground}} [\tilde{p}(\tau)]^2 \, d\tau. \quad (13)$$

Output Functional and Error

We consider the following output functional:

$$\mathcal{J}(\mathbf{u}) := \int_{\text{ground}} [\tilde{p}(\tau)]^2 \, d\tau. \quad (13)$$

We define output error as:

$$\varepsilon(\mathbf{u}_h) := \mathcal{J}(\mathbf{u}) - \mathcal{J}(\mathbf{u}_h). \quad (14)$$

For our nonlinear problem, the output error can be approximated using the **dual weighted residual** (DWR) method.

Output Functional and Error

We consider the following output functional:

$$\mathcal{J}(\mathbf{u}) := \int_{\text{ground}} [\tilde{p}(\tau)]^2 d\tau. \quad (13)$$

We define output error as:

$$\varepsilon(\mathbf{u}_h) := \mathcal{J}(\mathbf{u}) - \mathcal{J}(\mathbf{u}_h). \quad (14)$$

For our nonlinear problem, the output error can be approximated using the **dual weighted residual** (DWR) method.

Needs **correction**⁴ for artificial viscosity term (asymptotically consistent).

⁴B. Couchman 2020

Residual Consistency

- We say a form \mathcal{R}^C is **consistent** if:

$$\mathcal{R}^C(\mathbf{v}, \mathbf{u}) = 0, \quad \forall \mathbf{v} \in \mathcal{V}, \quad (15)$$

where \mathbf{u} is the exact solution.

Residual Consistency

- We say a form \mathcal{R}^C is **consistent** if:

$$\mathcal{R}^C(\mathbf{v}, \mathbf{u}) = 0, \quad \forall \mathbf{v} \in \mathcal{V}, \quad (15)$$

where \mathbf{u} is the exact solution.

- We say a form \mathcal{R}^A is **asymptotically consistent** if:

$$\mathcal{R}^A(\mathbf{v}, \mathbf{u}) = \mathcal{O}(h^\alpha), \quad \forall \mathbf{v} \in \mathcal{V}, \quad (16)$$

where \mathbf{u} is the exact solution, $\alpha > 0$, and h is a characteristic element size in \mathcal{T}_h .

Residual Consistency

- We say a form \mathcal{R}^C is **consistent** if:

$$\mathcal{R}^C(\boldsymbol{v}, \boldsymbol{u}) = 0, \quad \forall \boldsymbol{v} \in \mathcal{V}, \quad (15)$$

where \boldsymbol{u} is the exact solution.

- We say a form \mathcal{R}^A is **asymptotically consistent** if:

$$\mathcal{R}^A(\boldsymbol{v}, \boldsymbol{u}) = \mathcal{O}(h^\alpha), \quad \forall \boldsymbol{v} \in \mathcal{V}, \quad (16)$$

where \boldsymbol{u} is the exact solution, $\alpha > 0$, and h is a characteristic element size in \mathcal{T}_h .

In our situation:

$$\mathcal{R}(\boldsymbol{v}_h, \boldsymbol{u}_h) := \underbrace{\mathcal{R}^C(\boldsymbol{v}_h, \boldsymbol{u}_h)}_{:= \mathcal{R}^{CG}} + \underbrace{\mathcal{R}^A(\boldsymbol{v}_h, \boldsymbol{u}_h)}_{:= \mathcal{R}^{AV}}. \quad (17)$$

Dual Problem and Error for Linear Case

We assume linear residual and output functional, and define the **dual** (adjoint) problem as:

Find $\psi \in \mathcal{W}$ such that:

$$\mathcal{R}(\psi, \mathbf{w}) - \mathcal{J}(\mathbf{w}) = 0, \quad \forall \mathbf{w} \in \mathcal{W}. \quad (18)$$

Dual Problem and Error for Linear Case

We assume linear residual and output functional, and define the **dual** (adjoint) problem as:

Find $\psi \in \mathcal{W}$ such that:

$$\mathcal{R}(\psi, \mathbf{w}) - \mathcal{J}(\mathbf{w}) = 0, \quad \forall \mathbf{w} \in \mathcal{W}. \quad (18)$$

From there:

$$\begin{aligned}\varepsilon(\mathbf{u}_h) &= \mathcal{J}(\mathbf{u}) - \mathcal{J}(\mathbf{u}_h) \quad (\Delta\mathbf{u} := \mathbf{u} - \mathbf{u}_h) \\ &= \mathcal{J}(\Delta\mathbf{u})\end{aligned}$$

(19)

Dual Problem and Error for Linear Case

We assume linear residual and output functional, and define the **dual** (adjoint) problem as:

Find $\psi \in \mathcal{W}$ such that:

$$\mathcal{R}(\psi, \mathbf{w}) - \mathcal{J}(\mathbf{w}) = 0, \quad \forall \mathbf{w} \in \mathcal{W}. \quad (18)$$

From there:

$$\begin{aligned}\varepsilon(\mathbf{u}_h) &= \mathcal{J}(\mathbf{u}) - \mathcal{J}(\mathbf{u}_h) \quad (\Delta\mathbf{u} := \mathbf{u} - \mathbf{u}_h) \\ &= \mathcal{J}(\Delta\mathbf{u}) \\ &= \mathcal{R}(\psi, \Delta\mathbf{u})\end{aligned}$$

(19)

Dual Problem and Error for Linear Case

We assume linear residual and output functional, and define the **dual** (adjoint) problem as:

Find $\psi \in \mathcal{W}$ such that:

$$\mathcal{R}(\psi, \mathbf{w}) - \mathcal{J}(\mathbf{w}) = 0, \quad \forall \mathbf{w} \in \mathcal{W}. \quad (18)$$

From there:

$$\begin{aligned}\varepsilon(\mathbf{u}_h) &= \mathcal{J}(\mathbf{u}) - \mathcal{J}(\mathbf{u}_h) \quad (\Delta\mathbf{u} := \mathbf{u} - \mathbf{u}_h) \\ &= \mathcal{J}(\Delta\mathbf{u}) \\ &= \mathcal{R}(\psi, \Delta\mathbf{u}) \\ &= \underbrace{\mathcal{R}^C(\psi, \mathbf{u}) + \mathcal{R}^A(\psi, \mathbf{u})}_{=0} - \underbrace{\mathcal{R}^C(\psi, \mathbf{u}_h) + \mathcal{R}^A(\psi, \mathbf{u}_h)}_{=-\mathcal{R}(\psi, \mathbf{u}_h)}\end{aligned}$$

(19)

Dual Problem and Error for Linear Case

We assume linear residual and output functional, and define the **dual** (adjoint) problem as:

Find $\psi \in \mathcal{W}$ such that:

$$\mathcal{R}(\psi, \mathbf{w}) - \mathcal{J}(\mathbf{w}) = 0, \quad \forall \mathbf{w} \in \mathcal{W}. \quad (18)$$

From there:

$$\begin{aligned}
 \varepsilon(\mathbf{u}_h) &= \mathcal{J}(\mathbf{u}) - \mathcal{J}(\mathbf{u}_h) \quad (\Delta\mathbf{u} := \mathbf{u} - \mathbf{u}_h) \\
 &= \mathcal{J}(\Delta\mathbf{u}) \\
 &= \mathcal{R}(\psi, \Delta\mathbf{u}) \\
 &= \underbrace{\mathcal{R}^C(\psi, \mathbf{u})}_{=0} + \mathcal{R}^A(\psi, \mathbf{u}) - \underbrace{\mathcal{R}^C(\psi, \mathbf{u}_h)}_{=-\mathcal{R}(\psi, \mathbf{u}_h)} - \mathcal{R}^A(\psi, \mathbf{u}_h) \\
 &= -[\mathcal{R}(\psi, \mathbf{u}_h) - \mathcal{R}^A(\psi, \mathbf{u})] \quad (\text{Dual weighted residual error expression}) \tag{19}
 \end{aligned}$$

Approximations: DWR Error Estimate

So far:

$$\varepsilon(\mathbf{u}_h) = -[\mathcal{R}(\psi, \mathbf{u}_h) - \mathcal{R}^A(\psi, \mathbf{u})]. \quad (20)$$

Approximations: DWR Error Estimate

So far:

$$\varepsilon(\mathbf{u}_h) = -[\mathcal{R}(\psi, \mathbf{u}_h) - \mathcal{R}^A(\psi, \mathbf{u})]. \quad (20)$$

Issues:

- Primal exact solution \mathbf{u} is not available.
- Residual and output functional are in general nonlinear.
- Even if they are linear, adjoint exact solution ψ is not available.

Approximations: DWR Error Estimate

So far:

$$\varepsilon(\mathbf{u}_h) = -[\mathcal{R}(\psi, \mathbf{u}_h) - \mathcal{R}^A(\psi, \mathbf{u})]. \quad (20)$$

Issues:

- Primal exact solution \mathbf{u} is not available.
- Residual and output functional are in general nonlinear.
- Even if they are linear, adjoint exact solution ψ is not available.

First approximation:

$$\mathcal{R}^A(\psi, \mathbf{u}) \approx \mathcal{R}^A(\psi, \mathbf{u}_h), \quad (21)$$

justified on a shock dominated problem with AV.

Approximations: DWR Error Estimate

Second approximation:

ψ is approximated with a numerical adjoint $\psi_{\hat{h}}$ defined by⁵:

⁵M. Yano and D. L. Darmofal 2012

Approximations: DWR Error Estimate

Second approximation:

ψ is approximated with a numerical adjoint $\psi_{\hat{h}}$ defined by⁵:
 $\psi_{\hat{h}} \in \mathcal{V}_{\hat{h}, \hat{p}}$ such that:

$$\mathcal{R}'[\mathbf{u}_h](\psi_{\hat{h}}, \tilde{\mathbf{u}}) - \mathcal{J}'[\mathbf{u}_h](\tilde{\mathbf{u}}) = 0, \quad \forall \tilde{\mathbf{u}} \in \mathcal{V}_{\hat{h}, \hat{p}}, \quad (22)$$

where:

- $\mathcal{R}'[\mathbf{u}_h]$ and $\mathcal{J}'[\mathbf{u}_h]$ are the linearizations of \mathcal{R} and \mathcal{J} about \mathbf{u}_h .
- $\tilde{\mathbf{u}}$ represents a perturbation from \mathbf{u}_h .
- The space $\mathcal{V}_{\hat{h}, \hat{p}}$ contains polynomials of order $\hat{p} = p + 1$.

Approximations: DWR Error Estimate

Second approximation:

ψ is approximated with a numerical adjoint $\psi_{\hat{h}}$ defined by⁵:
 $\psi_{\hat{h}} \in \mathcal{V}_{\hat{h}, \hat{p}}$ such that:

$$\mathcal{R}'[\mathbf{u}_h](\psi_{\hat{h}}, \tilde{\mathbf{u}}) - \mathcal{J}'[\mathbf{u}_h](\tilde{\mathbf{u}}) = 0, \quad \forall \tilde{\mathbf{u}} \in \mathcal{V}_{\hat{h}, \hat{p}}, \quad (22)$$

where:

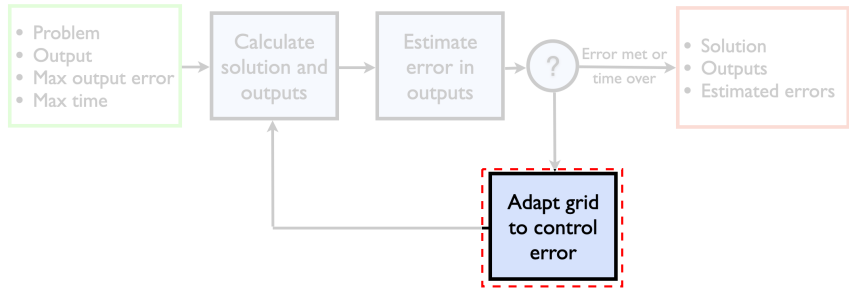
- $\mathcal{R}'[\mathbf{u}_h]$ and $\mathcal{J}'[\mathbf{u}_h]$ are the linearizations of \mathcal{R} and \mathcal{J} about \mathbf{u}_h .
- $\tilde{\mathbf{u}}$ represents a perturbation from \mathbf{u}_h .
- The space $\mathcal{V}_{\hat{h}, \hat{p}}$ contains polynomials of order $\hat{p} = p + 1$.

Final DWR error estimate:

$$\varepsilon(\mathbf{u}_h) \approx - \left[\mathcal{R}(\psi_{\hat{h}}, \mathbf{u}_h) - \mathcal{R}^A(\psi_{\hat{h}}, \mathbf{u}_h) \right]. \quad (23)$$

⁵M. Yano and D. L. Darmofal 2012

Mesh Adaptation



Continuous Optimization: Mesh-Metric Duality

Want mesh producing the smallest output error indicator \mathcal{E} :

$$\hat{\mathcal{T}}_h = \arg \inf_{\mathcal{T}_h \in \mathbb{T}(\Omega)} \mathcal{E}(\mathcal{T}_h), \quad \mathcal{C}(\mathcal{T}_h) < C. \quad (24)$$

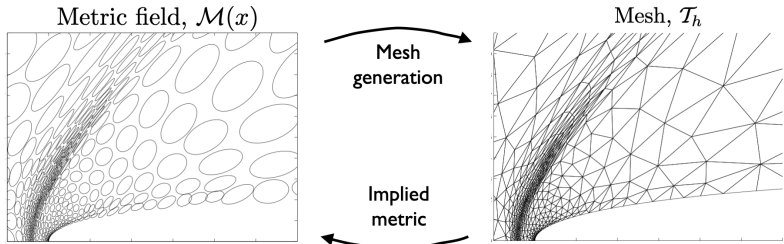
Continuous Optimization: Mesh-Metric Duality

Want mesh producing the smallest output error indicator \mathcal{E} :

$$\hat{\mathcal{T}}_h = \arg \inf_{\mathcal{T}_h \in \mathbb{T}(\Omega)} \mathcal{E}(\mathcal{T}_h), \quad \mathcal{C}(\mathcal{T}_h) < C. \quad (24)$$

Continuous relaxation⁶to address intractability of discrete problem.

$$\hat{\mathcal{M}} = \arg \inf_{\mathcal{M} \in \mathbb{M}(\Omega)} \mathcal{E}(\mathcal{M}), \quad \mathcal{C}(\mathcal{M}) < C \quad (25)$$



⁶A. Loseille and E. Alauzet 2011

MOESS⁸: Error Sampling and Synthesis

Need model for error indicator $\mathcal{E}(\mathcal{M})$: How \mathcal{E} changes with \mathcal{M} .

⁷T. Richter and T. Wick 2015

⁸M. Yano and D. L. Darmofal 2012

MOESS⁸: Error Sampling and Synthesis

Need model for error indicator $\mathcal{E}(\mathcal{M})$: How \mathcal{E} changes with \mathcal{M} .

First step: Compute nodal⁷ error indicators based on the DWR error estimate. Use partition of unity given by linear tent functions $\{\phi_v\}$.

⁷T. Richter and T. Wick 2015

⁸M. Yano and D. L. Darmofal 2012

MOESS⁸: Error Sampling and Synthesis

Need model for error indicator $\mathcal{E}(\mathcal{M})$: How \mathcal{E} changes with \mathcal{M} .

First step: Compute nodal⁷ error indicators based on the DWR error estimate. Use partition of unity given by linear tent functions $\{\phi_v\}$.

$$\varepsilon_v := -\mathcal{R}(\phi_v \Delta \psi_{\hat{h}}, \mathbf{u}_h) + \mathcal{R}^A(\phi_v \psi_{\hat{h}}, \mathbf{u}_h), \quad (26)$$

$$\eta_v := |\mathcal{R}(\phi_v \Delta \psi_{\hat{h}}, \mathbf{u}_h)| + |\mathcal{R}^A(\phi_v \psi_{\hat{h}}, \mathbf{u}_h)|, \quad \eta := \sum_v \eta_v \equiv \mathcal{E} \quad (27)$$

⁷T. Richter and T. Wick 2015

⁸M. Yano and D. L. Darmofal 2012

MOESS⁸: Error Sampling and Synthesis

Need model for error indicator $\mathcal{E}(\mathcal{M})$: How \mathcal{E} changes with \mathcal{M} .

First step: Compute nodal⁷ error indicators based on the DWR error estimate. Use partition of unity given by linear tent functions $\{\phi_v\}$.

$$\varepsilon_v := -\mathcal{R}(\phi_v \Delta \psi_{\hat{h}}, \mathbf{u}_h) + \mathcal{R}^A(\phi_v \psi_{\hat{h}}, \mathbf{u}_h), \quad (26)$$

$$\eta_v := |\mathcal{R}(\phi_v \Delta \psi_{\hat{h}}, \mathbf{u}_h)| + |\mathcal{R}^A(\phi_v \psi_{\hat{h}}, \mathbf{u}_h)|, \quad \eta := \sum_v \eta_v \equiv \mathcal{E} \quad (27)$$

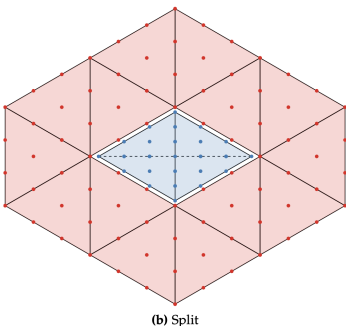
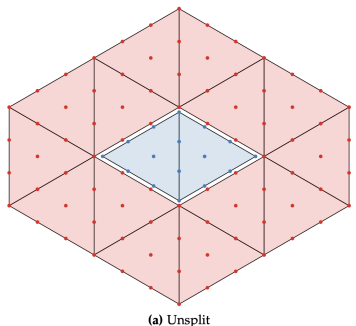
Next: Recompute solution and nodal indicators in refined *local patches* in the mesh.

The comparison of the nodal error indicators before and after the local solves gives information about how \mathcal{E} changes with \mathcal{M} .

⁷T. Richter and T. Wick 2015

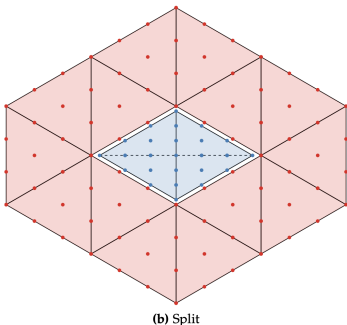
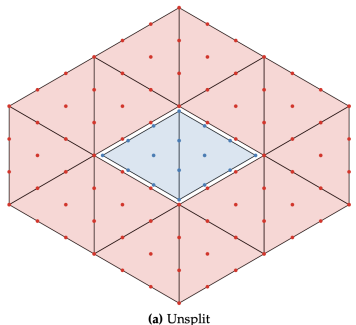
⁸M. Yano and D. L. Darmofal 2012

MOESS: Error Sampling and Synthesis



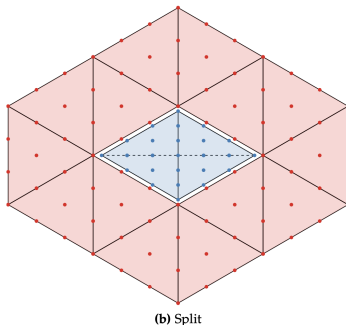
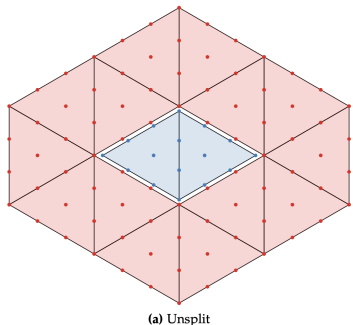
MOESS: Error Sampling and Synthesis

Local solve: Solve for $\mathbf{u}_h^\epsilon \in \mathcal{V}_{h,p}^\epsilon$ s.t. $\mathcal{R}_{\text{local}}(\mathbf{v}_h^\epsilon, \mathbf{u}_h^\epsilon) = 0, \quad \forall \mathbf{v}_h^\epsilon \in \mathcal{V}_{h,p}^\epsilon$.



MOESS: Error Sampling and Synthesis

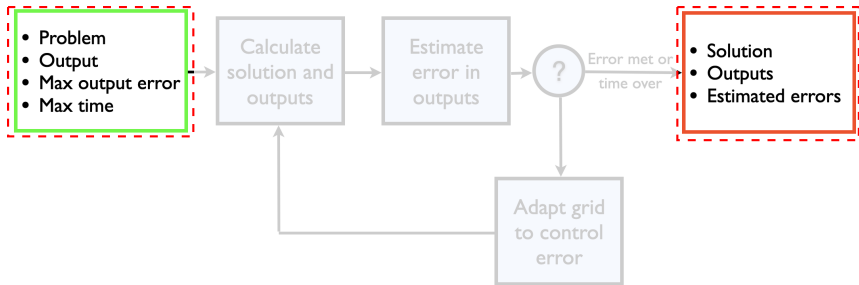
Local solve: Solve for $\mathbf{u}_h^\epsilon \in \mathcal{V}_{h,p}^\epsilon$ s.t. $\mathcal{R}_{\text{local}}(\mathbf{v}_h^\epsilon, \mathbf{u}_h^\epsilon) = 0, \quad \forall \mathbf{v}_h^\epsilon \in \mathcal{V}_{h,p}^\epsilon$.



Nodal indicator for vertices in inner patch:

$$\eta_v^\epsilon = |\mathcal{R}_{\text{local}}(\phi_v \Delta \psi_{\hat{h}}, \mathbf{u}_h^\epsilon)| + |\mathcal{R}_{\text{local}}^A(\phi_v \psi_{\hat{h}}, \mathbf{u}_h^\epsilon)|. \quad (28)$$

Results for Practical Case



Preliminary: Implementation Notes

Software: Solution Adaptive Numerical Simulator (SANS)⁹

- C++ framework to numerically solve partial differential equations.
- Supports several CG and DG discretizations, with output-based mesh adaptation.
- MPI parallelization.
- Unit testing and continuous integration.
- Open source.

⁹Galbraith et. al. 2015

Case Description

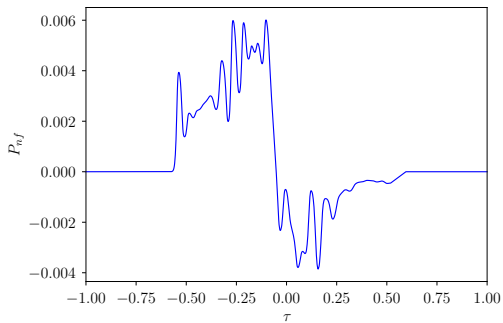
- Airplane Mach number: $M_a = 1.4$.
- Airplane altitude: $z_a = 16459.2$ m.
- Ground altitude: 110 m.



Source: lockheedmartin.com

Case Description

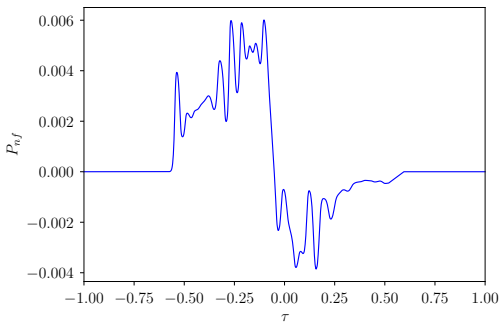
- Airplane Mach number: $M_a = 1.4$.
- Airplane altitude: $z_a = 16459.2$ m.
- Ground altitude: 110 m.
- Nearfield signal (initial condition):



Source: lockheedmartin.com

Case Description

- Airplane Mach number: $M_a = 1.4$.
- Airplane altitude: $z_a = 16459.2$ m.
- Ground altitude: 110 m.
- Nearfield signal (initial condition):

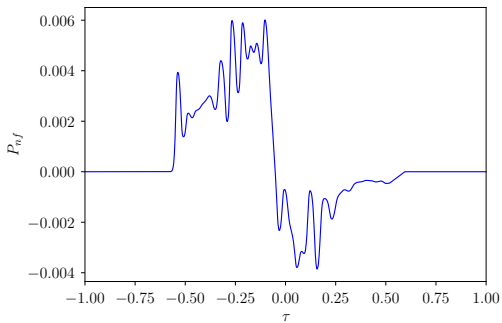


Source: lockheedmartin.com

- Domain dimensions:
 $\Omega = [-1, 2] \times [0, 257]$
- Output for adaptation:
 $\mathcal{J}_{BSEL} = \int_{\text{ground}} [\tilde{p}(\tau)]^2 d\tau$

Case Description

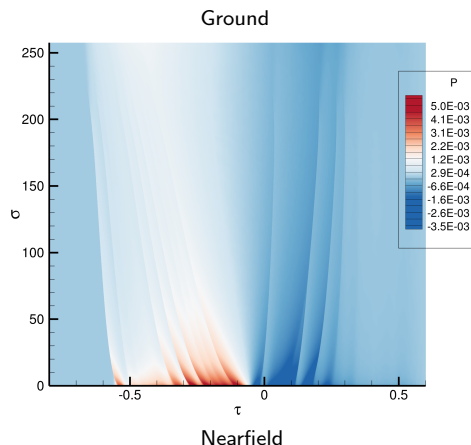
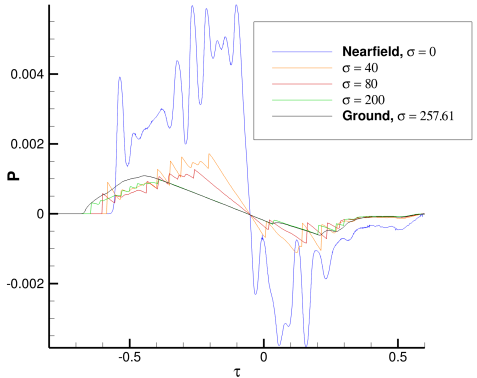
- Airplane Mach number: $M_a = 1.4$.
- Airplane altitude: $z_a = 16459.2$ m.
- Ground altitude: 110 m.
- Nearfield signal (initial condition):



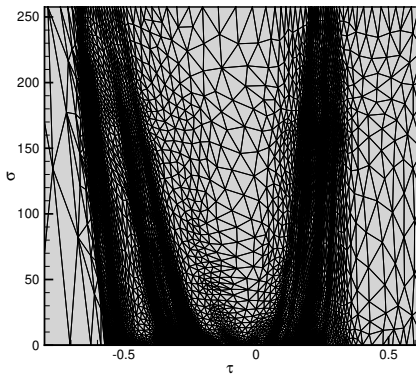
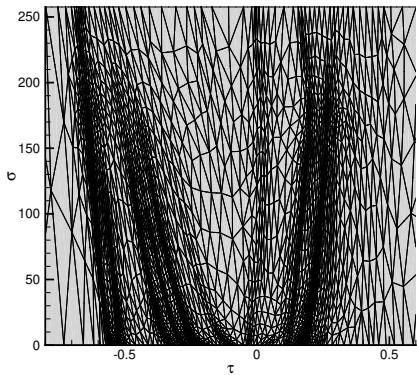
Source: lockheedmartin.com

- Domain dimensions:
 $\Omega = [-1, 2] \times [0, 257]$
- Output for adaptation:
 $\mathcal{J}_{BSEL} = \int_{\text{ground}} [\tilde{p}(\tau)]^2 d\tau$
- Also for comparison:
 $\mathcal{J}_p = \int_{\text{ground}} [p(\tau)]^2 d\tau$

Propagation: Pressure Perturbation Solution



Propagation: Final Adapted Mesh for 8K Target DOF

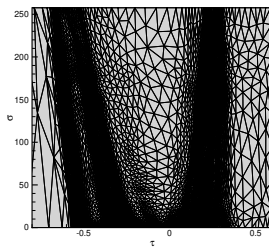
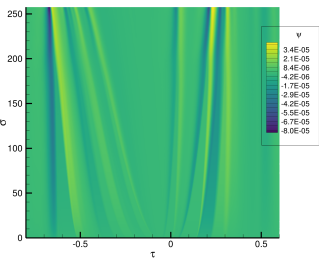
 $p = 1$  $p = 2$ 

Propagation: Evolution Over Adaptive Cycle, 8K Target DOF

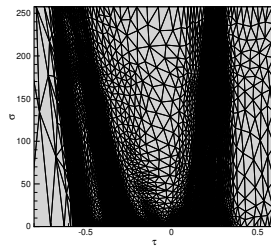
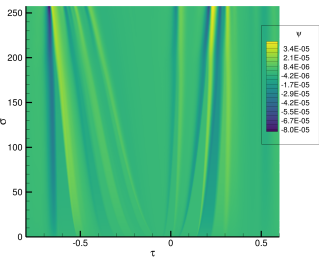
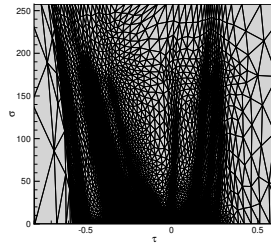
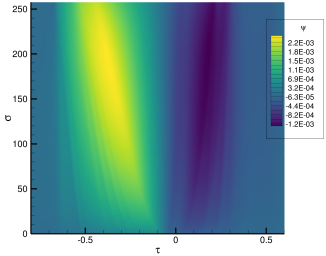


Different Adaptation Outputs and Their Adjoints

$\mathcal{J}_{\text{BSEL}}$

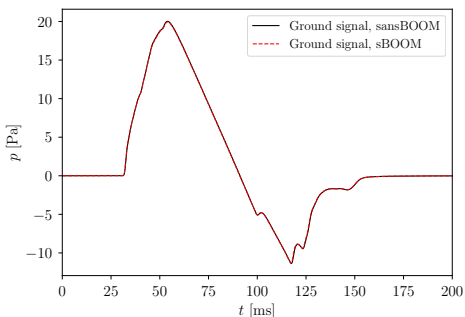


Different Adaptation Outputs and Their Adjoints

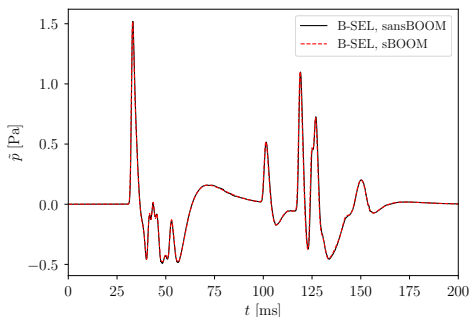
 \mathcal{J}_{BSEL}  \mathcal{J}_P 

At Ground: Pressure Signal and Its Filtering

Pressure Signal

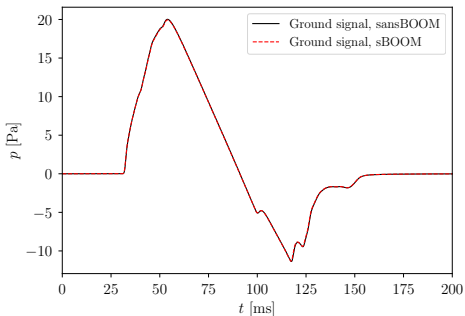


B-SEL Filter Output

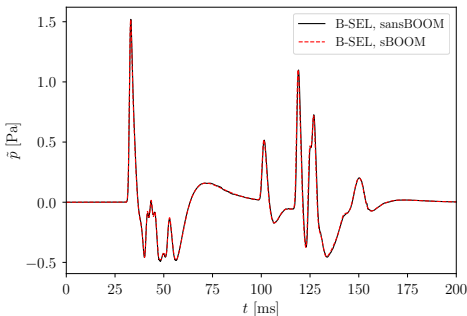


At Ground: Pressure Signal and Its Filtering

Pressure Signal



B-SEL Filter Output



Comparison with NASA *sBOOM* code¹⁰:

sansBOOM:

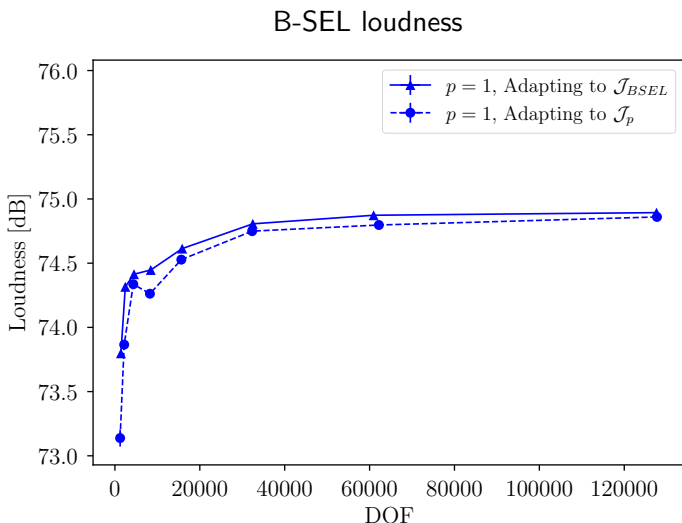
- Target of 128K DOF in total (space-time).
- Total DOF across the 40 adaptive iterations $\approx 3.2\text{M}$ DOF.

sBOOM (NASA, time-marching):

- 32K DOF in τ direction.
- 39K steps (marching) in σ direction.
- 1.2B DOF in total (space-time).

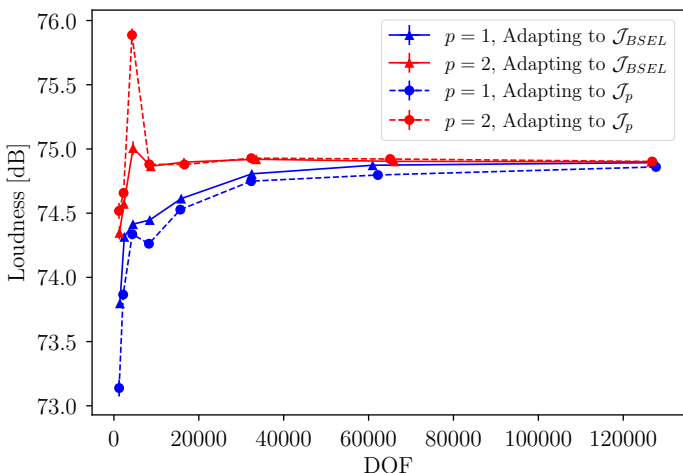
¹⁰S. K. Rallabhandi et. al. 2023

At Ground: Loudness Convergence with Mesh Refinement



At Ground: Loudness Convergence with Mesh Refinement

B-SEL loudness



Concluding Remarks

Work completed:

- Higher-order FEM to solve sonic boom propagation problem.
- Unstructured space-time mesh adaptation.
- Loudness error estimate driving mesh adaptation.

Concluding Remarks

Work completed:

- Higher-order FEM to solve sonic boom propagation problem.
- Unstructured space-time mesh adaptation.
- Loudness error estimate driving mesh adaptation.

Outcome:

- Significant reduction in space-time DOF count, at the expense of solving the optimization problem for the mesh.
- The above is highlighted when using higher-order solutions, as quadratic solutions converge the output faster than linear solutions.

Concluding Remarks

Work completed:

- Higher-order FEM to solve sonic boom propagation problem.
- Unstructured space-time mesh adaptation.
- Loudness error estimate driving mesh adaptation.

Outcome:

- Significant reduction in space-time DOF count, at the expense of solving the optimization problem for the mesh.
- The above is highlighted when using higher-order solutions, as quadratic solutions converge the output faster than linear solutions.

Ongoing effort:

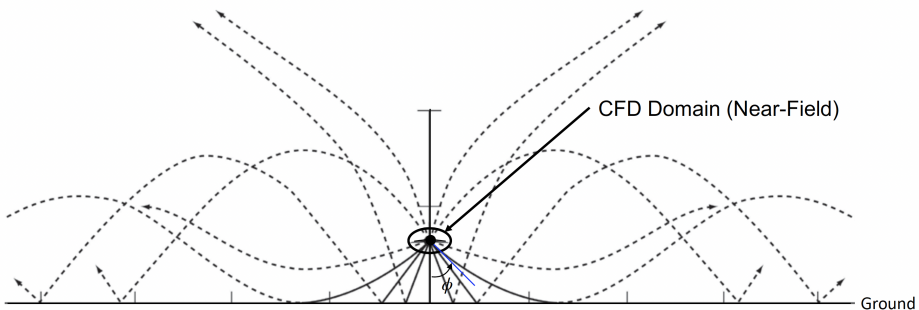
- Study convergence of loudness sensitivity to nearfield signal.

Acknowledgments

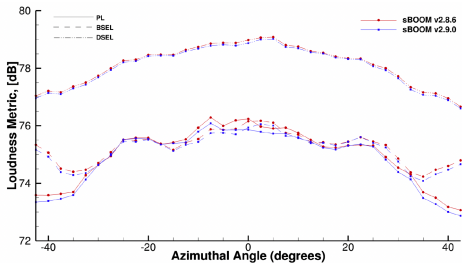
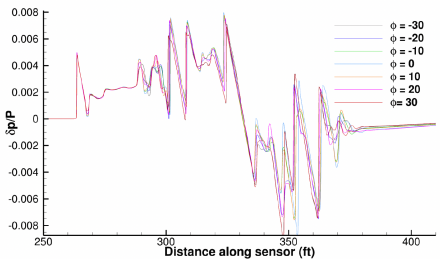
- This work was supported by funding from NASA (#80NSSC22K0193) with technical monitor Dr. Sriram Rallabhandi.
- The authors gratefully acknowledge technical assistance of NASA specifically from Sriram Rallabhandi, Michael Aftosmis, Marian Nemec, and David Rodriguez.

Thanks for the attention!
Questions?

Boom Carpet: Front View Schematic



Boom Carpet: Nearfield Conditions and Loudness Values¹¹

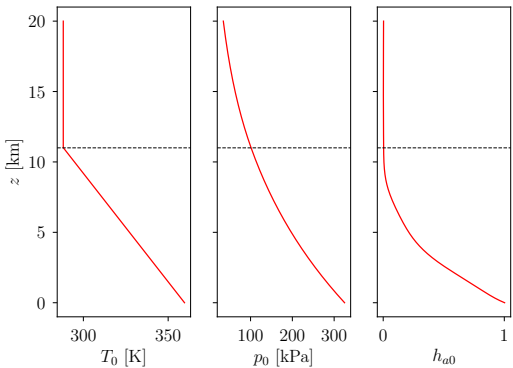


¹¹S. K. Rallabhandi et. al. 2023

Atmosphere Model: Standard

Atmosphere model refers to how the atmospheric properties depend on altitude.

Standard model: First two layers:



Additionally, models for:

- Density and speed of sound: ρ_0, c_0 ,
 - Gol'berg number: Γ ,
 - Relaxation coefficients: C_ν, θ_ν ,
 - Ray tube area: A_{n0} ,
- as functions of atmospheric properties.

Variational Multiscale with Discontinuous Subscales (VMSD) Method

Discretization of Ω :

$\mathcal{T}_h := \{\kappa\}_{\kappa=1}^K$ is a triangulation of the domain Ω into K elements.

Propose solution:

$$\mathbf{u}_h := \bar{\mathbf{u}}_{h,p} + \mathbf{u}'_{h,p'}, \quad \bar{\mathbf{u}}_{h,p} \in \bar{\mathcal{V}}_{h,p}, \quad \mathbf{u}'_{h,p'} \in \mathcal{V}'_{h,p'}.$$

VMSD solution spaces:

$$(Coarse scale) \quad \bar{\mathcal{V}}_{h,p} := \{\mathbf{v} \in [C^0(\Omega)]^m : \mathbf{v}|_\kappa \in [\mathcal{P}^p(\kappa)]^m, \forall \kappa \in \mathcal{T}_h\}, \quad (29)$$

$$(Fine scale) \quad \mathcal{V}'_{h,p'} := \{\mathbf{v} \in [L^2(\Omega)]^m : \mathbf{v}|_\kappa \in [\mathcal{P}^{p'}(\kappa)]^m, \forall \kappa \in \mathcal{T}_h\}. \quad (30)$$

Variational Multiscale with Discontinuous Subscales (VMSD) Method

Weak statement:

Find $(\bar{\mathbf{u}}_{h,p}, \mathbf{u}'_{h,p'}) \in \bar{\mathcal{V}}_{h,p} \times \mathcal{V}'_{h,p'}$ **such that:**

$$\mathcal{R}(\bar{\mathbf{v}}_{h,p}, \mathbf{v}'_{h,p'}; \bar{\mathbf{u}}_{h,p}, \mathbf{u}'_{h,p'}) = 0, \quad \forall (\bar{\mathbf{v}}_{h,p}, \mathbf{v}'_{h,p'}) \in \bar{\mathcal{V}}_{h,p} \times \mathcal{V}'_{h,p'}. \quad (31)$$

Remarks:

- $\mathbf{u}'_{h,p'}$ DOFs are element-wise decoupled. Thus, they can be static condensed and the total cost becomes the same as a CG method.
- For same accuracy requirement, more efficient (less DOFs) than CG and DG.
- Adjoint consistent.

Shock Indicator s_{grad}

Starting point:

$$\xi := \frac{H_{\tau\tau}}{p} \left| \frac{\partial P}{\partial \tau} \right|, \quad \hat{\xi} = \frac{\xi}{\xi_1}, \quad (32)$$

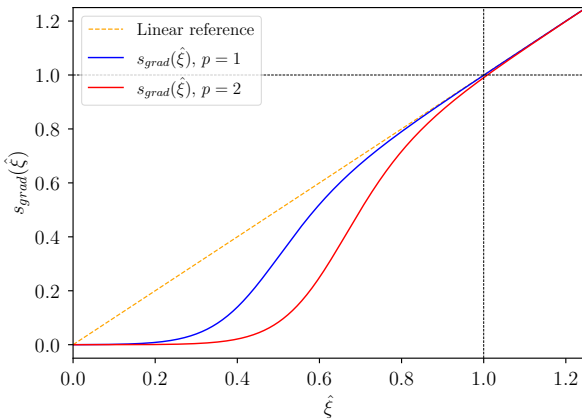
then:

$$s_{\text{grad}} := s_{\text{grad}}(\hat{\xi}) = \frac{\hat{\xi} [\tanh(p^2 \hat{\xi})]^{p-1}}{1 + \exp \left[-k (\hat{\xi} - \alpha(p)) \right]}, \quad (33)$$

where $k, \alpha(p) \in \mathbb{R}$.

Shock Indicator s_{grad}

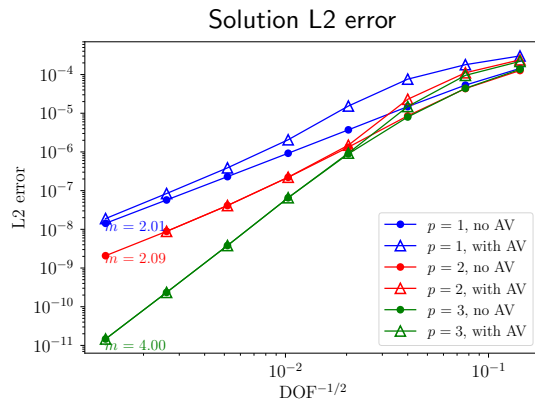
$$s_{\text{grad}} := s_{\text{grad}}(\hat{\xi}) = \frac{\hat{\xi}[\tanh(p^2\hat{\xi})]^{p-1}}{1 + \exp[-k(\hat{\xi} - \alpha(p))]}, \quad (34)$$



Test With Smooth Problem

Smooth problem with available exact solution:

- Solve without artificial viscosity.
- Solve with artificial viscosity and see how it affects convergence.



Run Summary

① Set:

- Case parameters and nearfield condition.
- Initial 2D mesh.
- Target DOF.
- Number of adaptive iterations (N).

② Loop, $i \in \{1, \dots, N\}$:

- Solve primal problem:
 - [Burgers system + shock sensor] in 2D mesh.
 - Filter ODE in ground boundary.
- Solve adjoint problem:
 - Adjoint ODE in ground boundary.
 - [Burgers system + shock sensor] adjoint in 2D mesh.
- Nodal error sampling and synthesis.
- Adapt mesh.

③ Average results:

- Average any quantity of interest (e.g. output value) over last n adaptive iterations.

Ongoing Effort: Loudness Sensitivity to Nearfield Signal

